

INFECTIOUS DISEASES

Evolution of inflammation and immunity in a dengue virus 1 human infection model

Adam T. Waickman^{1,2*}, Joseph Q. Lu^{1,2}, HengSheng Fang¹, Mitchell J. Waldran¹, Chad Gebo¹, Jeffrey R. Currier³, Lisa Ware², Liesbeth Van Wesenbeeck⁴, Nathalie Verpoorten⁴, Oliver Lenz⁴, Lotke Tambuyzer⁴, Guillermo Herrera-Taracena⁵, Marnix Van Lookk⁴, Timothy P. Endy¹, Stephen J. Thomas^{1,2}

Dengue virus (DENV) infections are major causes of morbidity and mortality throughout the tropics and subtropics. More than 400 million infections are estimated to occur every year, resulting in nearly 100 million symptomatic infections and more than 20,000 deaths. Early immune response kinetics to infection remain unclear, in large part due to the variable incubation period exhibited by the DENVs after introduction into a susceptible host. To fill this knowledge gap, we performed a comprehensive virologic and immunologic analysis of individuals experimentally infected with the underattenuated DENV-1 strain 45AZ5. This analysis captured both the kinetics and composition of the innate, humoral, and cellular immune responses elicited by experimental DENV-1 infection, as well as virologic and clinical features. We observed a robust DENV-specific immunoglobulin A (IgA) antibody response that manifested between the appearance of DENV-specific IgM and IgG in all challenged individuals, as well as the presence of a non-neutralizing/NS1-specific antibody response that was delayed relative to the appearance of DENV virion-specific humoral immunity. RNA sequencing analysis revealed discrete and temporally restricted gene modules that correlated with acute viremia and the induction of adaptive immunity. Our analysis provides a detailed description, in time and space, of the evolving matrix of DENV-elicited human inflammation and immunity and reveals several previously unappreciated immunological aspects of primary DENV-1 infection that can inform countermeasure development and evaluation.

INTRODUCTION

Dengue is caused by infection with any of the four dengue virus (DENV) serotypes (DENV-1 to DENV-4). The viruses are transmitted when an infected female *Aedes* mosquito takes a blood meal from a susceptible, nonimmune host (1). Each year, an estimated 400 million people, most living in tropical and subtropical regions, are thought to be infected, and about 100 million infections manifest with a range of clinical phenotypes (2, 3). About 500,000 dengue cases require hospitalization, and up to 20,000 people succumb to the disease every year (4). Dengue is expected to become a worsening global public health challenge because the main drivers of DENV transmission are projected to continue and/or accelerate over the next several decades (e.g., climate change, travel, population growth, poverty, and urbanization). It is estimated that by 2080, more than 6 billion people will live at daily risk of a DENV infection (5). A number of vaccines have been under development (6–9), but the single dengue vaccine currently available is limited to people 9 years of age and older and only for individuals who have preexisting dengue immunity (10–12). Although several promising candidates are in early-stage clinical development (13), there is no anti-DENV antiviral currently available for prophylaxis or as a therapeutic treatment. Despite more than a century of basic science research, countermeasure development

efforts, and attempts at vector control, dengue remains a largely unchecked public health burden.

Development of dengue countermeasures (i.e., drugs, vaccines, diagnostics, and vector control tools) has been hindered by fundamental gaps in our understanding of DENV transmission, pathogenesis, and anti-DENV immune responses. These knowledge gaps include understanding who is at risk of DENV exposure, why some infected people become ill and others do not, and what environmental and/or genetic factors increase infection risk. Addressing these knowledge gaps is critical to support countermeasure development efforts. Studying wild-type infections to answer these questions has been challenging for several reasons including the following: (i) the extreme difficulty of capturing people in the first few days after infection and before symptoms develop, (ii) the issue of many people living in dengue-endemic regions have preexisting DENV or non-DENV flavivirus immunity from past infections or vaccinations, and (iii) the difficulty of collecting blood samples at a frequency that allows for detailed kinetic analyses. For these reasons, our group has collaboratively developed an experimental dengue human infection model (DHIM) (14).

A DHIM has the potential to be a powerful tool for studying human host responses to DENV infection. Individuals with known preexisting flavivirus immune profiles are infected with a highly characterized and underattenuated DENV strain manufactured under good manufacturing practices and administered in a controlled clinical environment. The participants are intensely followed through the measurement of clinical, clinical laboratory, virologic, and immunologic responses over time. Experimental human infection with the DENVs have been documented since 1902 and have greatly contributed to our foundational

Copyright © 2022
The Authors, some
rights reserved;
exclusive licensee
American Association
for the Advancement
of Science. No claim
to original U.S.
Government Works

¹Department of Microbiology and Immunology, State University of New York Upstate Medical University, Syracuse, NY 13210, USA. ²Institute for Global Health and Translational Sciences, State University of New York Upstate Medical University, Syracuse, NY 13210, USA. ³Viral Diseases Branch, Walter Reed Army Institute of Research, Silver Spring, MD 20910, USA. ⁴Janssen Pharmaceutica, NV, Beerse, Belgium. ⁵Janssen Global Public Health, Janssen Research and Development, Horsham, PA 19044, USA.

*Corresponding author. Email: waickmaa@upstate.edu

understanding of DENV transmission, virology, and immunology (15–25). More recent studies have characterized the clinical and functional immune profiles after DENV-1 or DENV-2 infection, explored the early transcriptional features of attenuated DENV-2 infection, and described the cellular immune responses after infection (9, 14, 26–28). However, to date, no study has comprehensively and longitudinally sought to assess and integrate the virologic and immunologic parameters associated with a primary DENV infection in a flavivirus-naïve individual.

To this end, our team set out to thoroughly characterize the clinical, immunologic, and virologic features of a primary DENV-1 infection in flavivirus-naïve adults with fine temporal resolution. This analysis captured both the kinetics and composition of the innate, humoral, and cellular immune response elicited by experimental DENV-1 infection and the virologic and clinical features of infection.

RESULTS

Study overview and clinical outcome of DENV-1 infection

This study was conducted to characterize the longitudinal virologic and immunologic profile associated with a primary DENV-1 infection in flavivirus-naïve adults. To this end, nine participants (table S1) were enrolled to receive a single subcutaneous inoculation of 0.5 ml of a suspension [6.5×10^4 plaque-forming units (PFU)/ml] of the underattenuated DENV-1 strain 45AZ5 (14). This virus strain originated from a Chinese patient with mild dengue fever living on the island of Nauru (western Pacific) in 1974 and was subsequently serially passaged in a diploid fetal rhesus lung cell line (FRhL) and mutagenized with 5-azacytidine to facilitate the accumulation of attenuating mutations (29, 30).

Participants in this study were evaluated daily for the first 14 days after inoculation and then every other day until 28 days after virus inoculation, with additional visits on days 90 and 180 after inoculation. All nine enrolled participants completed the study per protocol and were included in the subsequent virologic and immunologic analyses.

Within 7 days after inoculation, five of nine participants reported at least one solicited local adverse event (AE) (injection site symptom). The five participants reporting solicited local AEs described mild (grade 1) reactions including bruising, discomfort, erythema, and injection site hemorrhage. No related unsolicited local AEs were reported. Within 28 days after inoculation, all nine participants reported at least one solicited systemic AE including headache, rash, fever, eye pain, weakness, and myalgia (Table 1 and table S2). Most participants (eight of nine) had at least one laboratory abnormality between study days 1 and 181, most of which were mild or moderate, and all were reported within 28 days after inoculation or 7 days after hospitalization, whichever was later (Table 1, fig. S1, and table S3). At least one severe laboratory abnormality was reported by three of the nine participants. One potentially life-threatening AE was observed (low serum glucose) but failed to correlate with the clinical presentation at the time of the routine follow-up visit and returned to normal levels by the following day. The abnormality was subsequently assessed by the principal investigator as unrelated to the viral challenge. As with previous studies, all participants who became ill were managed with oral fluids, acetaminophen, and an antinausea medication if required. No intravenous access was required.

All study participants developed detectable RNAemia and viremia as assessed by quantitative reverse transcription polymerase chain reaction (qRT-PCR) and Vero cell-based plaque assay,

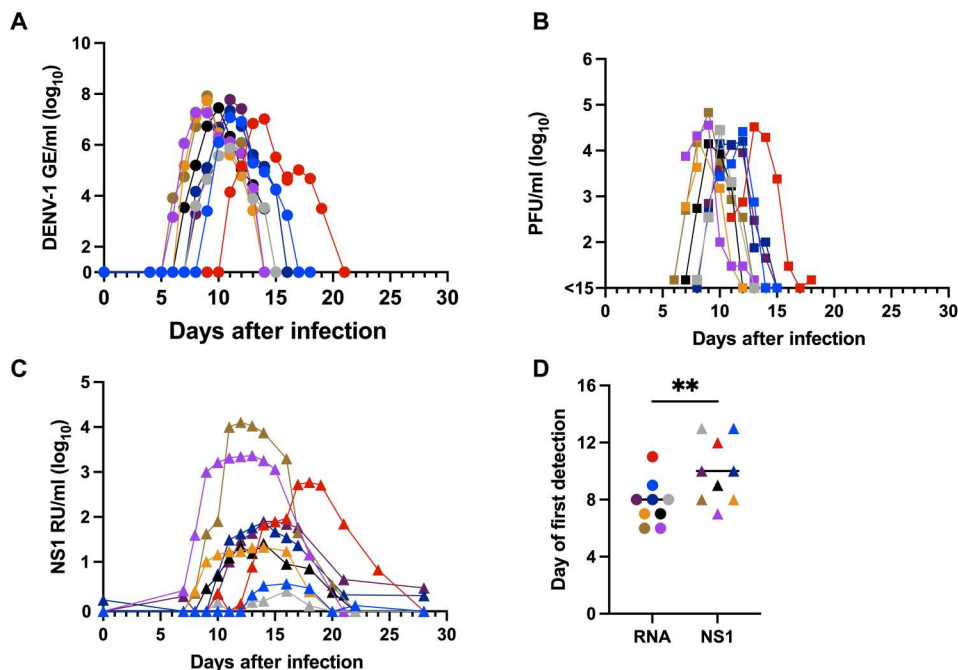


Fig. 1. Kinetics of DENV-1 infection in 45AZ5-challenged individuals. (A) DENV-1 RNA content in serum as assessed by qRT-PCR. (B) Infectious DENV-1 content in serum as assessed Vero cell plaque assay. (C) NS1 protein content in serum as assessed by ELISA. (D) Comparison of RNAemia and NS1 antigenemia onset in all study participants. ****** $P < 0.01$, paired t test. The line indicates group median.

Table 1. DHIM performance parameters. ALT, alanine transaminase; AST, aspartate transaminase.

Participants experiencing:	All participants (N = 9) n/M (%)
Measurable RNAemia of 3 to 11 days duration	9/9 (100)
Fever measured at least two times in 24 hours but not lasting more than 72 hours	5/9 (55.6)
At least one of the following symptoms	9/9 (100)
At least two of the following symptoms	8/9 (88.9)
Fever and at least one of the following symptoms	5/9 (55.6)
Fever and at least two of the following symptoms	4/9 (44.4)
Headache, maximum grade 1 or 2	8/9 (88.9)
Myalgia, maximum grade 1 or 2	7/9 (77.8)
Rash, maximum grade 1 or 2	5/9 (55.6)
Liver function tests (ALT and AST), maximum grade 1 or 2	3/9 (33.3)
Leukopenia, maximum grade 1 or 2	6/9 (66.7)
Thrombocytopenia, maximum grade 1 or 2	1/9 (11.1)

respectively, with a largely uniform viral kinetics pattern (Fig. 1, A and B, and fig. S2). The incubation period (time from infection to detectable RNAemia) ranged from 6 to 11 days, with RNAemia persisting for a mean of 8 days. Peak viral load ranged from 7.46×10^5 to 8.33×10^7 genome equivalents (GE)/ml or 1.3×10^4 to 6.8×10^4 PFU/ml of serum. In addition to circulating virus, DENV NS1 antigenemia was detected as early as day 7 after inoculation (range of 7 to 13 days), with NS1 antigenemia persisting for a mean of 13 days across all study participants (Fig. 1C). When compared to RNAemia as quantified by qRT-PCR, the levels of NS1 serum antigenemia exhibited more variability between participants and appeared, on average, 2 days later than viral RNA (Fig. 1D).

Kinetics and specificity of DENV-1–elicited humoral immunity

Having established the kinetics of DENV-1 RNAemia, viremia, and antigenemia after 45AZ5 infection, we next assessed the induction of DENV-1–specific humoral immunity. Although induction of immunoglobulin M (IgM) or IgG isotype antibodies is most commonly used for serological confirmation of DENV infection and for monitoring durable antiviral immunity, we included IgA in our analysis given our previous observation that primary DENV infection is associated with a substantial IgA response and may have an association with disease severity (31, 32). Using a previously described virion-capture enzyme-linked immunosorbent assay (ELISA), we observed a robust but transient DENV-1–specific IgM and IgA response in all participants, with IgM and IgA seroconversion occurring on average by postinfection days 14 and 16, respectively (Fig. 2, A and B). All participants still exhibited detectable anti-DENV-1 IgM titers at day 90 after DENV-1 challenge, whereas only three of nine participants maintained an IgA titer. DENV-1–specific IgG seroconversion occurred later than IgM or IgA in all participants, with detectable DENV-1–specific IgG

appearing on average by day 19 after infection and remaining stable out to 90 days after infection (Fig. 2, A and B).

In light of the robust NS1 antigenemia observed after 45AZ5 infection, we additionally assessed the kinetics and magnitude of anti-NS1–specific humoral immunity. Similar to our observations with the DENV-1 virion capture assay, DENV-1 NS1–specific IgM/IgA responses after 45AZ5 infection were transient, whereas IgG levels persisted and remained elevated out to day 90 after infection (Fig. 2C). Although not statistically significant, a DENV-1 NS1–specific IgM/IgA response occurred earlier (on average on days 19 and 20, respectively) when compared to IgG responses, which appeared by day 23 on average (Fig. 2D). When comparing DENV virion specific with DENV-1 NS1–specific humoral immune response, antiviral immunity tended to appear earlier (average seroconversion was between days 14 and 19 for the antiviral response versus days 19 and 23 for the anti-NS1 response) (Fig. 2, B and D), thus resembling the pattern observed for the appearance of DENV-1 virions and NS1 antigen.

NS1 is predominantly secreted as a hexamer by flavivirus-infected cells, but the protein can also be found on the cellular plasma membrane in a dimeric configuration (33, 34). The biological function of surface-restricted NS1 is unclear, but the antigen can facilitate opsonization of infected cells by NS1-reactive antibodies, thereby allowing NK cells, monocytes, and other phagocytic cells to recognize and clear infected cells via Fc receptor–mediated mechanisms such as antibody-dependent cellular cytotoxicity and antibody-dependent cellular phagocytosis (35, 36). To measure the abundance of opsonizing NS1-specific antibodies, we used a CEM.NK^R cell line that was engineered to stably express DENV-1 NS1 (fig. S3) and quantified the abundance of anti-NS1–opsonizing antibodies using flow cytometry. As was observed for the antihexameric NS1 antibody titers, induction of opsonizing anti-NS1 IgM and IgA isotype antibodies was transient after inoculation, with IgG isotype responses appearing later and persisting through day 90 after infection (Fig. 2E). The average day of opsonizing anti-NS1 seroconversion was day 18 (IgM), day 20 (IgA), and day 21 (IgG) (Fig. 2F), further emphasizing the delayed kinetics of anti-NS1 immunity relative to virion-specific humoral immunity.

Kinetics and specificity of DENV-1–elicited cellular immunity

To define the magnitude and specificity of DENV-1–elicited cellular immunity after 45AZ5 infection, peripheral blood mononuclear cells (PBMCs) collected from all study participants on study days 0, 28, and 90 were stimulated with overlapping peptide pools spanning the E, NS1, NS3, and NS5 proteins of DENV-1 and analyzed in an interferon- γ (IFN- γ) enzyme-linked immunosorbent spot (ELISpot) assay (table S4). As has been described after natural DENV infection or inoculation with a live attenuated vaccine product (37, 38), infection with 45AZ5 resulted in the generation of DENV-1–specific cellular immunity, as assessed by IFN- γ ELISpot, by 28 days after infection, which remained elevated out to day 90 after infection (Fig. 3A and fig. S4). DENV-1 NS3 was the dominant antigen recognized on days 28 and 90 after infection (Fig. 3, B and C, and fig. S4), followed in magnitude by E, NS5, and NS1.

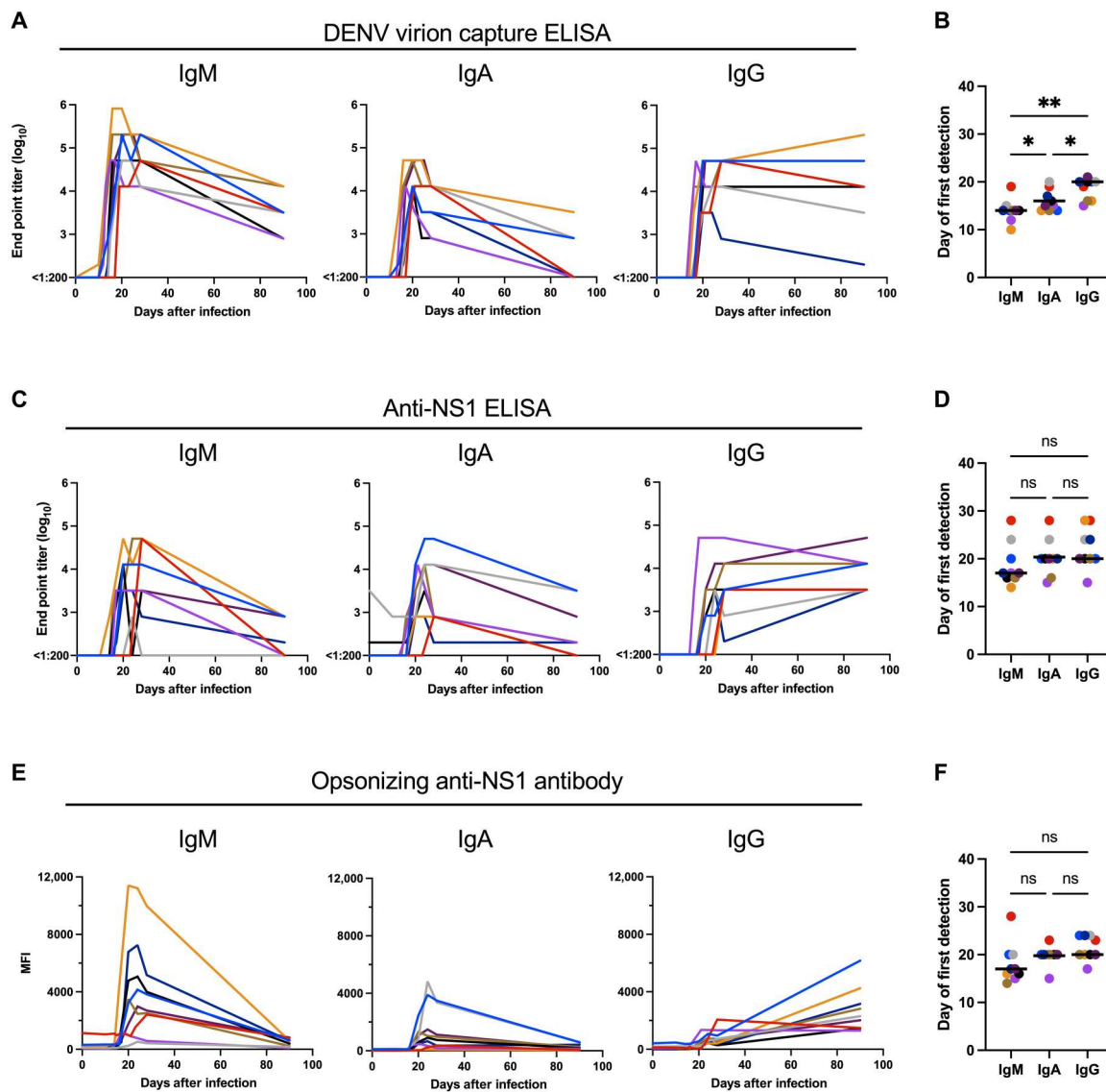


Fig. 2. Kinetics and characteristics of DENV-1 specific humoral immunity after 45AZ5 infection. (A) Antibody end point titers using virion-capture ELISA. (B) Day of DENV virion-specific seroconversion by antibody isotype. $*P < 0.05$ and $**P < 0.01$, paired one-way analysis of variance (ANOVA) with correction for multiple comparisons. (C) Antibody end point titers using NS1 protein ELISA. (D) Day of anti-NS1 seroconversion by antibody isotype. ns, not significant. (E) Opsonizing anti-NS1 antibody staining using NS1-expressing CEM.NK^R cells. MFI, mean fluorescence intensity. (F) Day of opsonizing anti-NS1 seroconversion by antibody isotype

Transcriptional analysis of DENV-elicited inflammation

The marked serologic and cellular immune responses elicited by 45AZ5 infection led us to better define the early kinetic profile of DENV-1-elicited inflammation. Previous studies have examined the transcriptional profile associated with acute natural DENV infection and have identified conserved gene signatures that correlate with disease severity (39). However, the inability of these studies to precisely define the day of DENV infection means that the timing and nature of the earliest transcriptional response to DENV infection are unclear.

To address this, we performed RNA sequencing (RNAseq) analysis on whole blood collected on study days 0, 8, 10, 14, and 28 from all nine study participants. These study days were selected on the basis of previous single-cell RNAseq (scRNAseq) analysis of a

select number of participants enrolled in a separate DENV-1 experimental infection study, which demonstrated that these days would likely capture both the early innate/inflammatory signatures associated with acute DENV infection and the subsequent activation and expansion of DENV-reactive lymphocytes (26).

Consistent with our previously published results, only modest and inconsistent transcriptional perturbations from baseline were observed across study participants on day 8 after infection. However, a marked transcriptional shift away from the preinfection profile was observed on days 10 and 14 after infection, with all participants demonstrating a return to baseline by day 28 after infection (Fig. 4A). No statistically significant differentially expressed genes (DEGs) were observed on days 8 and 28 relative to day 0. However, 112 genes (110 up-regulated and 2 down-regulated)

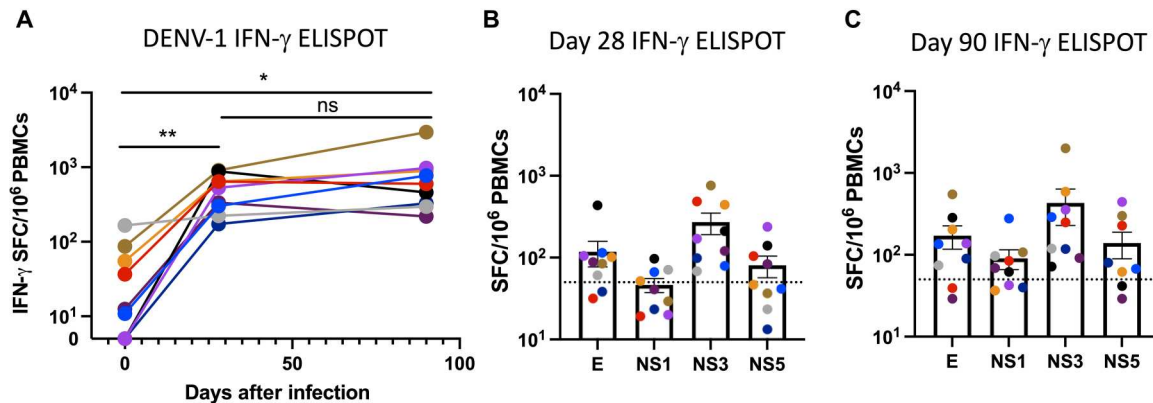


Fig. 3. Kinetics and specificity of DENV-1-elicited cellular immunity. (A) Total DENV-1-specific cellular immunity as assessed by IFN- γ ELISPOT. Sum of background-subtracted E, NS1, NS3, and NS5 reactivity at each indicated time point. * $P < 0.05$ and ** $P < 0.01$, paired one-way ANOVA with correction for multiple comparisons. (B) Antigen-specific breakdown of day 28 DENV-1-specific cellular immunity. (C) Antigen-specific breakdown of day 90 DENV-1-specific cellular immunity. Dashed line indicates 50 SFC/10⁶ PBMCs.

were observed to be differentially expressed on day 10 after infection (Fig. 4B and tables S5 and S6), whereas 177 genes (151 up-regulated and 26 down-regulated) were differentially expressed on day 14 relative to preinfection (Fig. 4C and tables S7 and S8).

The DEGs observed on day 10 after infection included many canonical IFN-stimulated and antiviral gene products (MX1, IFIT1, PARP9, and IFI44), whereas the day 14 DEG additionally included genes associated with lymphocyte proliferation and antibody production and functionalization (MKI67, TYMS, JCHAIN, and C1QC) (tables S9 and S10). There was a significant overlap between the DEG observed on days 10 and 14 after 45AZ5 infection, mostly restricted to gene products associated with type I IFN signaling and response to viral ligands (table S11). Consistent with the clinical profile associated with 45AZ5 experimental infection, there was no overlap between the DEGs captured in this study and a previously published gene set curated to identify participants with an increased risk of progressing to severe dengue (Fig. 4D) (39). Gene Ontology (GO) analysis performed on the DEGs identified on days 10 and 14 after infection indicated that most of the gene products differentially expressed on day 10 after 45AZ5 infection corresponded to pathways associated with acute/innate immune responses to viral infection (Fig. 4E), whereas those genes differentially expressed on day 14 after infection also included terms associated with lymphocyte activation and the induction of an adaptive immune response (Fig. 4E).

Kinetic DENV-elicited inflammation and lymphocyte activation

Having identified DEG on days 10 and 14 after DENV-1 infection, we next sought to better describe the functional kinetics of DENV-1-elicited inflammation and DENV-specific immunity using these transcriptional profiles. The day 14 DEG contained gene products that corresponded to both type I IFN signaling and virus sensing (IFI27, IFI44L, and GBP1), as well as genes associated with lymphocyte activation and proliferation (MKI67, TYMS, JCHAIN, and MZB1).

Leveraging the functional heterogeneity of the transcriptional profile observed on day 14 after 45AZ5 challenge, we endeavored to reduce the dimensionality of the RNAseq dataset in such a way

that allowed for the unbiased identification of biologically relevant metrics of infection. Accordingly, the expression of the genes highlighted as being differentially expressed on day 14 was assessed across all time points in all samples, and the resulting expression matrix subjected to unsupervised/hierarchical clustering to identify groups of genes that exhibited coordinated expression across all time points and samples.

Using this approach, three distinct gene modules were identified within the aggregated dataset (Fig. 5A and table S12). Gene module 1 identified in this analysis consisted of gene products associated with cellular proliferation and lymphocyte activation (Fig. 5, A and B, and tables S12 and S13), whereas gene module 2 preferentially contained genes associated with type I/II IFN signaling, virus sensing, and defense responses to viruses (Fig. 5, A and B, and tables S12 and S14). Gene module 3 consisted of genes that were suppressed on day 14 relative to day 0 after infection but do not appear to fall into any biologically consistent category (table S12).

To better visualize the expression kinetics of the genes contained within the two modules highlighted in this analysis, we calculated a module 1 and module 2 score for every sample. The module score was defined as the sum of the normalized abundance transcripts per million (TPM) of the genes contained within a module in a given sample. The expression of genes found in module 1 or module 2 was exclusive across the time points captured in this analysis, with the expression of the inflammation-associated module 2 preceding the expression of the lymphocyte-associated module 1 in all participants (Fig. 5, C and D). The preferential expression of module 2 genes on days 8 and 10 after infection corresponds to the window of viremia observed in this study, whereas the expression of module 1 genes reflects the anticipated timing of B cell activation after primary DENV-1 infection.

To further confirm that module 1 expression corresponds to B cell activation, we leveraged the fact that activated/antibody-secreting B cells contain ~1000 \times the number of Ig transcripts as resting naïve/memory B cells. We assembled and annotated the unique immunoglobulin heavy chain (IGH) clones contained within our un-enriched/untargeted RNAseq libraries. This analysis indicated that the number of unique antibody clones captured in our data was significantly elevated on day 14 relative to all other time points

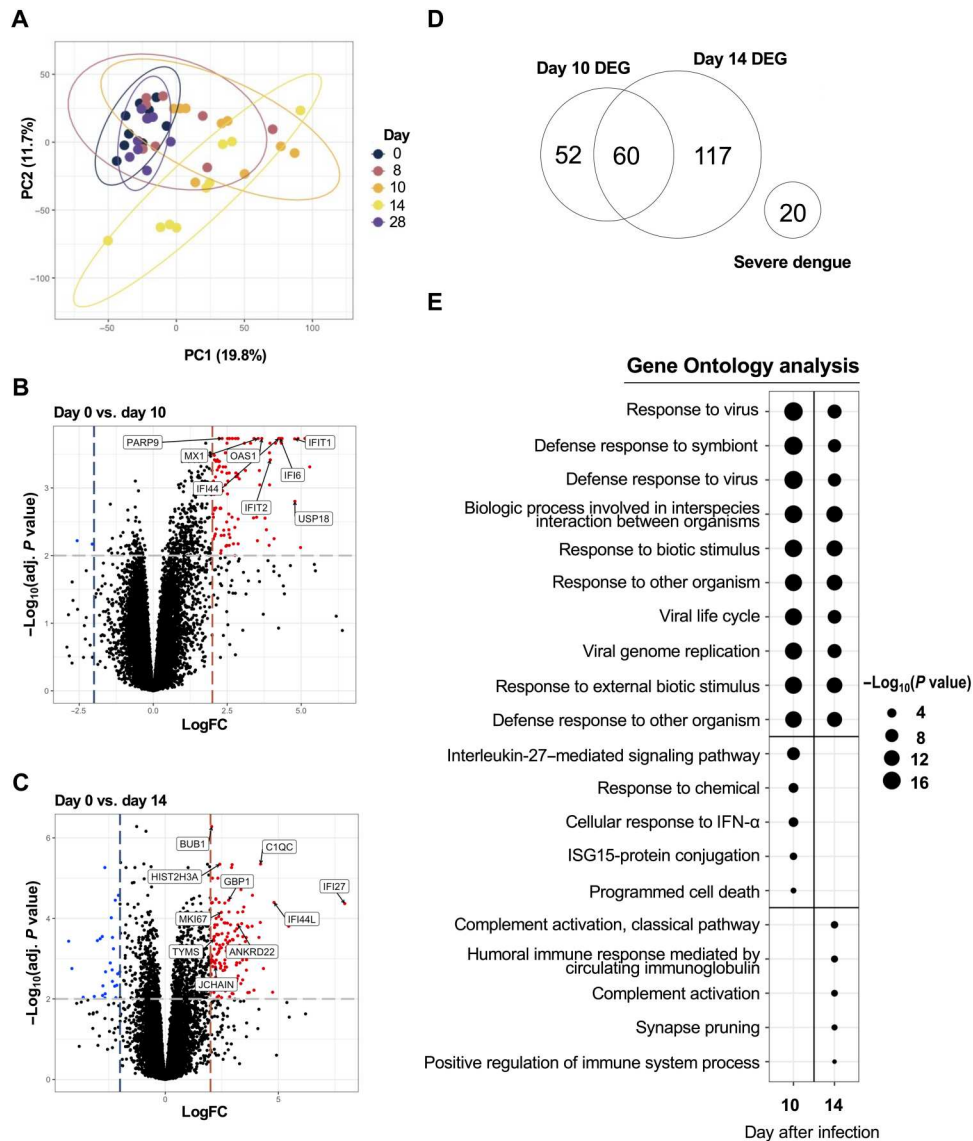


Fig. 4. Kinetics and composition of DENV-1-elicited inflammation. (A) Principal components (PC) analysis plot of RNAseq analysis of whole blood obtained on days 0, 8, 10, 14, and 28 after DENV-1 infection. Points are colored by sample collection day. (B) Volcano plot showing differential gene expression day 0 versus day 10 post-infection, with select statically and biologically significant genes highlighted. Genes with a log₂ fold change of >2 and an adjusted P value of <0.01 were considered significant. (C) Volcano plot showing differential gene expression day 0 versus day 14 postinfection, with select statically and biologically significant genes highlighted. Genes with a log₂ fold change of >2 and an adjusted P value of <0.01 were considered significant. (D) Overlap of Differentially expressed genes (DEGs) observed on days 10 and 14 and relationship to genes previously described to correlate with a progression to severe dengue. (E) Gene Ontology (GO) analysis of gene differentially expressed on days 10 and 14 relative to day 0 after DENV-1 infection. Highlighted are the 10 most statistically significant GO terms observed in the DEG sets from both days 10 and 14 postinfection, the 5 most significant GO terms observed only on day 10, and the 5 most significant GO terms observed only on day 14

(Fig. 5E). Not all participants exhibited a module 1 and IGH clone peak on day 14, suggesting either that these participants did not experience a significant adaptive response to DENV-1 infection or that the peak of lymphocyte activation occurred outside of our analysis window. In their totality, these data demonstrate the presence of temporally distinct and dynamic gene modules that evolve after DENV-1 infection and can be used to infer the magnitude of inflammation and timing after DENV-1 infection.

Evolution of DENV-elicited immunity and correlation between virologic and immunologic features of DENV-1 infection

To add context to the virologic and immunologic parameter captured in this analysis and to explore potential causal relationships with clinically relevant end points, we next examined the relative timing and correlative relationships between the individual components captured in this analysis. We selected 11 virologic and immunologic parameters and calculated the probability of observing a positive signal for a given feature within a 4- to 5-day window

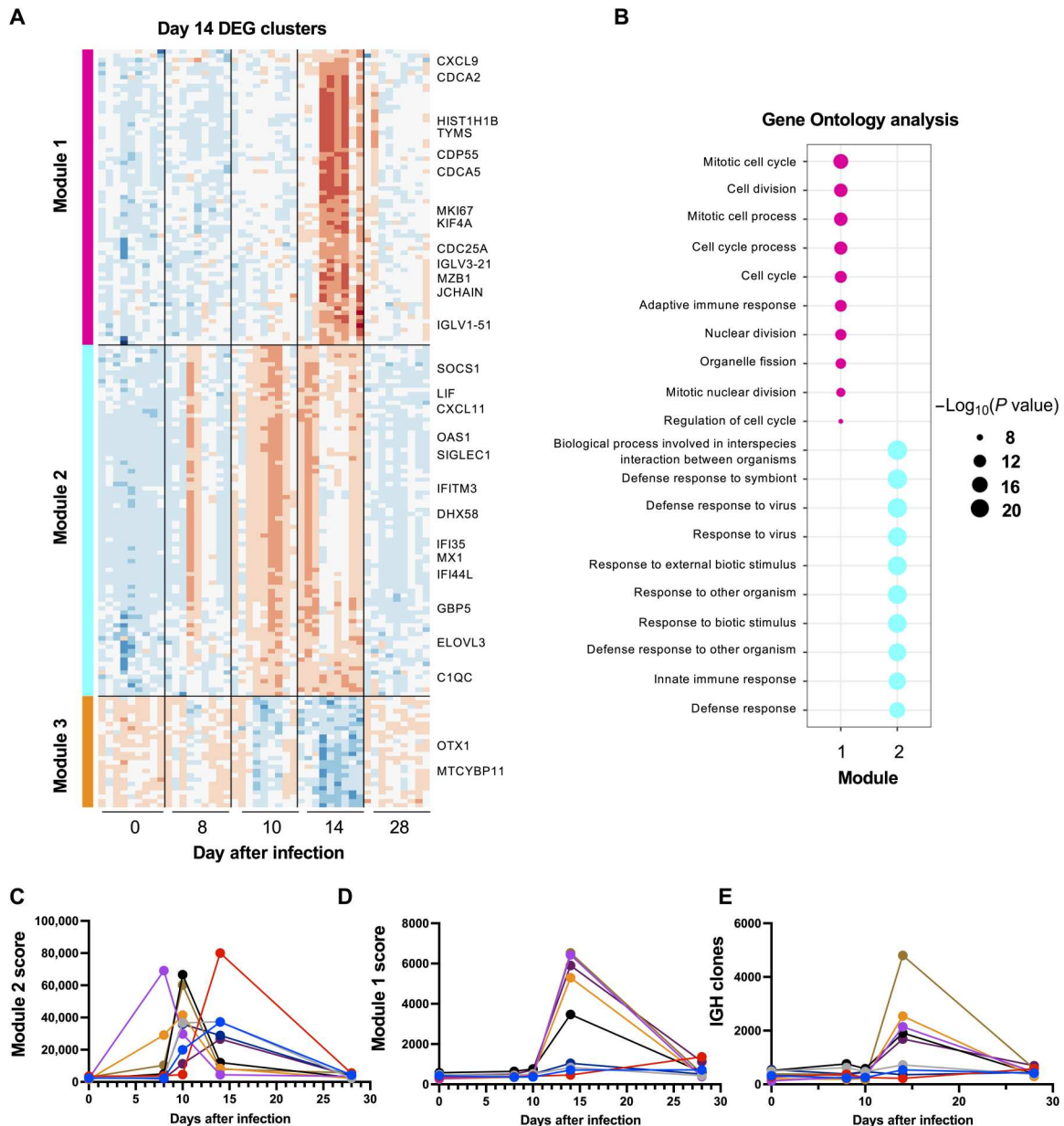


Fig. 5. Identification, characterization, and timing of DENV-1-elicited inflammation and lymphocyte activation. (A) Identification of coordinated gene modules among genes differentially express on day 14 versus day 0, with select biologically significant genes highlighted. (B) Gene ontology (GO) analysis of the genes found in module 1 and module 2. The 10 most statistically significant GO terms are highlighted for each module. (C) Kinetics of module 2 expression across all nine study participants and five time points. (D) Kinetics of module 1 expression across all nine study participants and five time points. (E) Identification and quantification of unique IGH clones across all nine study participants and five time points from the unenriched RNAseq data using MiXCR.

between 0 and 30 days after DENV-1 infection (Fig. 6A). Placed in context, the delayed appearance of NS1 antigen relative to DENV viral RNA is mirrored by a corresponding delay in the appearance of NS1-specific antibodies relative to virion-specific antibodies. However, a conserved progression of IgM, IgA, and IgG seroconversion is observed for antibodies targeting both viral antigens. The probability of observing the inflammation-associated RNAseq-derived gene module 2 coincides with the appearance of viral RNA and is immediately followed by the appearance of the lymphocyte activation-associated gene module 1, the time of DENV

virion-specific seroconversion. The inflammation-associated gene module 2 can be detected before the window during which fever was observed in study participants.

The day of RNAemia onset correlated notably with the appearance of NS1 antigenemia and the day of RNAseq-defined inflammation (Fig. 6B). Furthermore, the onset of RNAemia correlated with the timing of IgM and IgA seroconversion, but less well with the appearance of either DENV virion or NS1-specific IgG. The only immunologic parameter that inversely correlated with the magnitude of DENV RNAemia and the abundance of NS1

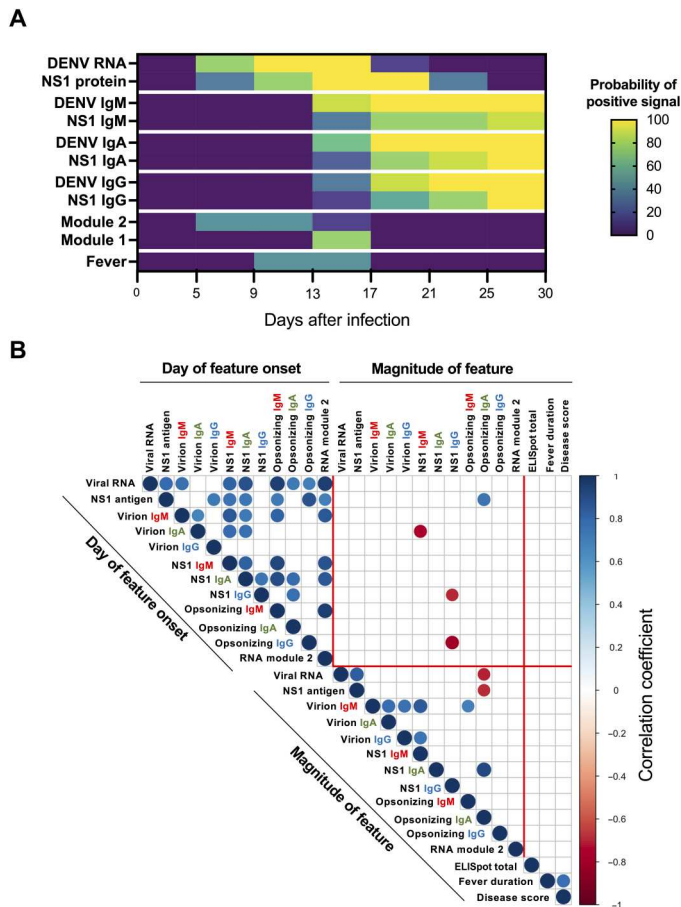


Fig. 6. Summary and correlation of DENV-elicited inflammation and immunity. (A) Aggregate summary of the timing of DENV proliferation and immune response. (B) Pearson's correlation of all virologic and immunologic parameters quantified in this study. Point size and color indicate strength and direction of correlation. Point size and color indicates strength and direction of correlation. Empty squares indicate $P > 0.05$.

antigen was the abundance of NS1 opsonizing IgA antibody, although the clinical relevance of this observation is unclear. In its totality, these data suggest that the kinetics of DENV-1-elicited inflammation and immunity in this human challenge model are largely driven by the timing of RNAemia, but that the absolute abundance of viral antigen does not necessarily directly correlate with the magnitude of the subsequent DENV-specific immune response.

DISCUSSION

In this study, we characterized the clinical, immunologic, and virologic features of primary DENV-1 infection in flavivirus-naïve adults. This analysis captured both the kinetics and composition of the innate, humoral, and cellular immune responses elicited by experimental DENV-1 infection, as well as the virologic and clinical features of DENV-1 infection in nine individuals inoculated with the underattenuated DENV-1 strain 45AZ5. The induction of both DENV virion-specific humoral immunity and anti-NS1-specific immunity was monitored, along with the induction and

antigen specificity of DENV-specific cellular immunity. Furthermore, extensive RNAseq analysis was performed on whole blood collected from study participants throughout the course of DENV-1 infection.

Several notable immunological features of primary DENV-1 infection are revealed in this analysis, most notably the robust IgA response targeting both DENV virions and DENV NS1. The presence of DENV- and NS1-specific serum IgA has previously been described after both natural primary and secondary DENV infection (32, 40–42), but the kinetics and relative magnitude of these responses were previously unclear. The timing of IgA seroconversion is notable, because the fact that it appears between IgM and IgG seroconversion makes the developmental origin of the IgA-secreting B cells somewhat ambiguous. Our previous analysis of B cells circulating after natural DENV infection demonstrated that Igs expressed by DENV-elicited/IgA-expressing plasmablasts were heavily hypermutated (32). This suggests that these IgA class-switched cells may be derived from previously activated and hypermutated memory B cells even after primary DENV infections. The putative memory B cell origin of the DENV-reactive IgA is strengthened by the kinetics of IgA seroconversion observed in our study, as the appearance of DENV-reactive IgA only lags IgM seroconversion by a few days and precedes the appearance of DENV-specific IgG.

Although IgA-biased immune responses have canonically been associated with mucosal pathogen infection, more recent analyses have shown a key IgA component after infection with other nonmucosal pathogens (such as malaria) and after mRNA vaccination (43, 44). This raises the possibility that a cross-reactive IgA response is an intrinsic feature of any immune response and may draw upon the clonal diversity represented in the normally mucosal-restricted immune system to speed antibody secretion upon the introduction of a new nonmucosal pathogen. Furthermore, the transient nature of circulating DENV-specific IgA isotype antibodies observed in our study has several interesting epidemiological implications. The presence of DENV/NS1-specific IgA may be a more temporally sensitive indication of recent DENV infection than IgM or IgG alone.

Dissecting the transcriptional profile associated with acute DENV infection and identifying transcriptional signatures that correlate with clinical outcome of infection has been a longstanding goal in the dengue community (26, 27, 39). Hanley *et al.* (27) provided insight into the kinetics of the inflammatory transcriptional program elicited by infection with the National Institutes of Health (NIH) rDEN2Δ30 strain and additionally identified preinfection transcriptional signatures that correlated with the clinical outcomes of infection, including the development of rash after infection. However, note that the DENV-1 45AZ5 DENV-1 strain used in our study generated 100- to 1000-fold higher levels of viremia than the rDEN2Δ30 strain and resulted in a broader range of dengue-like symptoms, including fever. Accordingly, the more robust clinical response to 45AZ5 infection appears to be accompanied by a quantitatively and qualitatively more vigorous inflammatory response than is observed after rDEN2Δ30 infection. When coupled with the extensive sampling performed in our analysis, the reactivity and immunogenicity of 45AZ5 allowed for the identification, characterization, and head-to-head comparison of the innate/inflammatory response to acute DENV infection and the subsequent adaptive immune response. The extensive RNAseq analysis performed in this study allowed for the

identification and characterization of discrete gene modules that track with acute viral-elicited inflammation and the onset of adaptive immunity after infection. Although preliminary, this high-resolution map of the immunologic trajectory of uncomplicated/mild dengue may allow for more accurate and unbiased assessment of the clinical trajectory of patients experiencing natural dengue.

The DHIM tool was designed to recapitulate the human natural infection experience and allow the early interrogation of potential countermeasures before advancing to field trials. Although participants do experience dengue-like symptoms, clinical laboratory abnormalities, viral replication, and immune responses consistent with natural infection, it is important to note a few dissimilarities. It is unclear what viral dose a mosquito delivers to a susceptible host during the feeding process. In our trial, we deliver a consistent and standardized dose that may or may not reflect what is delivered in nature. The mosquito proboscis probes a relatively superficial anatomic space in the skin as it searches for blood-filled capillaries. In the DHIM, we use a needle to deliver the virus into the subcutaneous space, a method that may produce a different antigen-processing pathway than what occurs in nature. Mosquitoes deliver wild-type viruses; in the DHIM, we use viruses that have been attenuated through cell passage or chemical exposure, and in the DHIM, we do not mix the virus with mosquito saliva before injection, which is different than the natural feeding process. Future DHIM iterations may address these differences.

In conclusion, we have demonstrated the ability to safely and consistently experimentally infect people with an underattenuated DENV strain and generated a mild dengue-like illness manifesting with clinical signs and symptoms, clinical laboratory abnormalities, and virologic and immunologic immune responses consistent with natural DENV infections. The immune response to this underattenuated DENV appears to be consistently most robust between days 10 and 14 after infection, suggesting that these days may warrant additional/focused analysis in the future. These studies not only provide insights into previously underappreciated immune responses but also underscore the potential value of the DHIM tool in supporting anti-dengue countermeasure development.

MATERIALS AND METHODS

Study design

The DHIM and associated analysis were approved by the State University of New York Upstate Medical University (SUNY-UMU) and the Department of Defense's Human Research Protection Office. This phase 1, open-label study (ClinicalTrials.gov identifier: NCT03869060) is an expansion of a previous study evaluating a dengue 1 live virus human infection (DENV-1-LVHC) model (ClinicalTrials.gov identifier: NCT02372175) (14). The study was conducted between March 2019 and February 2021 at the SUNY-UMU in Syracuse, NY. Participants were recruited from the Syracuse, NY area and neighboring cities via Institutional Review Board-approved posters, email, radio advertisements, social media outlets, word of mouth, site database, and a recruiting agency.

Nine participants received a single subcutaneous inoculation of 3.25×10^3 PFU of the 45AZ5 DENV-1 infection strain virus manufactured at the Walter Reed Army Institute of Research (WRAIR) Pilot Bioproduction Facility, Silver Spring, MD (U.S. Food and Drug Administration Investigational New Drug 16332). All

participants were prescreened to ensure the absence of preexisting flavivirus using the Euroimmun dengue, West Nile, and Zika IgG ELISA kits (Lübeck, Germany). The 45AZ5 DENV-1 infection strain used in this study was generated by a serial passage of the parental Nauru/West Pac/1974 DENV-1 isolate through diploid FRhL in the presence of 5-azacytidine, followed by plaque cloning and secondary amplification in FRhL cells (30, 45). Quantitative DENV-1-specific RT-PCR was performed using previously published techniques (46). Serum NS1 antigen levels were quantified using a Euroimmun dengue NS1 ELISA kit (Lübeck, Germany). For samples that were over the limit of quantification of the assay at the recommend dilution, samples were rerun at a 1:4 to 1:100 dilutions. All data points were graphed on the basis of standard curve accounting for the dilution factor, with an upper extinction coefficient of 5000 relative unit (RU)/ml. The day of NS1 antigenemia onset was defined as the day at which there was a detectable NS1 titer that persisted for more than 1 day.

DENV-1 virion-capture ELISA

DENV-1-reactive serum IgM/IgA/IgG levels were assessed using a flavivirus-capture ELISA protocol. In short, 96-well Nunc MaxSorp flat-bottom plates were coated with flavivirus group-reactive mouse monoclonal antibody 4G2 (2 µg/ml) (Envigo Bioproducts Inc.) diluted in borate saline buffer. Plates were washed and blocked with 0.25% bovine serum albumin and 1% normal goat serum in phosphate-buffered saline (PBS) after overnight incubation. DENV-1 (strain Nauru/West Pac/1974) was captured for 2 hours, followed by extensive washing. Serum samples were fourfold serially diluted and plated in duplicate and incubated for 1 hour at room temperature on the captured virus. DENV-specific IgM/IgG/IgA levels were quantified using anti-human IgM horseradish peroxidase (HRP) (SeraCare, 5220-0328), anti-human IgG HRP (SouthernBiotech, 2044-0), and anti-human IgA HRP (BioLegend, 411,002). Secondary antibody binding was quantified using the TMB Microwell Peroxidase Substrate System (KPL, catalog no. 50-76-00) and Synergy HT plate reader. DENV-1 (strains Nauru/West Pac/1974) was propagated in Vero cells and purified by ultracentrifugation through a 30% sucrose solution. End point titers were determined as the reciprocal of the final dilution at which the optical density (OD) was greater than 3× of a control flavivirus-naïve serum. The day of seroconversion was defined as the day at which a participant's end point titer exceeded that of their respective day 0 sample.

Anti-NS1 ELISA

To quantify DENV-1 NS1-reactive serum IgM/IgA/IgG antibodies levels, 96-well Nunc MaxSorp flat-bottom plates were coated with DENV-1 NS1 protein (2 µg/ml) (Native Antigen) diluted in carbonate/bicarbonate buffer and incubated overnight at 4°C. Serum samples were fourfold serially diluted, plated, and incubated for 2 hours at room temperature. DENV-1 NS1-specific IgM/IgG/IgA levels were quantified using anti-human IgM HRP (SeraCare, 5220-0328), anti-human IgG HRP (SouthernBiotech, 2044-0), and anti-human IgA HRP (BioLegend, 411,002). Secondary antibody binding was quantified using the TMB Microwell Peroxidase Substrate System (KPL, catalog no. 50-76-00) and Synergy HT plate reader. End point titers were determined as the reciprocal of the final dilution at which the OD was greater than 2× of a control flavivirus-naïve serum. The day of seroconversion was defined as the

day at which a participant's end point titer exceeded that of their respective day 0 sample.

Anti-NS1 opsonization assay

DENV-1 NS1 expressing CEM.NK^R cells (fig. S3) were stained with a 1:500 dilution of heat-inactivated serum diluted in PBS at room temperature for 30 min. Cells were extensively washed and then stained with goat anti-human IgA AF647 (2050-31, SouthernBiotech), goat anti-human IgG AF467 (2040-31, SouthernBiotech), or goat anti-human IgM AF647 (2020-31, SouthernBiotech). Flow cytometry analysis was performed on a BD LSR II instrument, and data were analyzed using FlowJo v10.2 software (Treestar). Reported mean fluorescence intensity (MFI) values are background-subtracted, with the background defined as the signal observed staining DENV-1 NS1-expressing CEM.NK^R cells in the absence of serum. The day of seroconversion was defined as the day at which a participant's background-subtracted NS1-specific MFI increased by at least 2× over their respective day 0 value.

IFN-γ ELISpot

Cryopreserved PBMCs were thawed, washed twice, and placed in RPMI 1640 (Corning, Tewksbury, MA, USA) supplemented with 10% heat-inactivated fetal calf serum (Corning, 35-010-CV), L-glutamine (Lonza, Basel, Switzerland), and penicillin/streptomycin (Gibco, Waltham, MA, USA). Cellular viability was assessed by trypan blue exclusion, and cells were resuspended at a concentration of 5×10^6 /ml and rested overnight at 37°C. After resting, viable PBMCs were washed, counted, and resuspended at a concentration of 1×10^6 /ml in complete cell culture medium. Next, 100 μl of this cell suspension was mixed with 100 μl of the individual peptide pools listed in table S4 and diluted to a final concentration 1 μg/ml per peptide [dimethyl sulfoxide (DMSO) concentration of 0.5%] in complete cell culture media. This cell and peptide mixture was loaded onto a 96-well polyvinylidene difluoride plate coated with anti-IFN-γ (3420-2HW-Plus, Mabtech, Nacka, Sweden) and cultured overnight. Controls for each participant included 0.5% DMSO alone (negative) and anti-CD3 (positive). After overnight incubation, the ELISpot plates were washed and stained with anti-IFN-γ-biotin followed by streptavidin-conjugated HRP (3420-2HW-Plus, Mabtech). Plates were developed using a TMB substrate and read using a CTL-ImmunoSpot S6 analyzer (Cellular Technology Limited, Shaker Heights, OH, USA). All peptide pools were tested in duplicate, and the adjusted mean was reported as the mean of the duplicate experimental wells after subtracting the mean value of the negative (DMSO only) control wells. Individuals were considered reactive to a peptide pool when the background-subtracted response was >50 spot-forming cells (SFC)/10⁶ PBMCs. All data were normalized on the basis of the number of cells plated per well and are presented here as SFC/10⁶ PBMCs.

RNAseq library preparation and sequencing

Whole blood was collected from all study participants using PAXgene RNA collection tubes (BD Biosciences) and frozen at -20°C until analyzed. RNA was recovered from the collection tubes using the QIAGEN PAXgene Blood RNA Isolation Kit and sequencing libraries created using Illumina Stranded Total RNA Prep with Ribo-Zero Plus and IDT-Ilmn RNA UD Indexes Set A. Final library quality control (QC) and quantification were performed using a Bioanalyzer (Agilent) and DNA 1000 reagents.

Libraries were pooled at an equimolar ratio and sequenced on a 300-cycle NovaSeq 6000 instrument using v1.5 S4 reagent set.

RNAseq gene expression analysis

Raw reads from FASTQ files were mapped to the human reference transcriptome (Ensembl, *Homo sapiens*, GRCh38) using Kallisto version 0.46.2 (47). Transcript-level counts and abundance data were imported and summarized in R (version 4.0.2) using the TxImport package (48) and TMM normalized using the package EdgeR (49, 50). Differential gene expression analysis was performed using linear modeling and Bayesian statistics in the R package Limma (51). Genes with a log₂ fold change of >2 and a Benjamini-Hochberg adjusted *P* value of <0.01 were considered significant. Gene Ontology (GO) analysis was performed using the gprofiler2 package (52). Gene module scores were calculated by summing the TMM normalized abundance (TPM) of the genes highlighted as belonging to either module 1 or module 2 for all samples. Gene module expression was considered positive when the module score for a given subject exceed 2× the day 0 score.

B cell receptor clonotype identification and annotation

Raw FASTQ files were filtered to contain only pair-end reads and to remove any Illumina adaptor contamination and low-quality reads using Trimmomatic (v0.39) (53). Pair-end reads were subsequently analyzed using MiXCR (v3.0.3) using the RNAseq/nontargeted genomic analysis pipeline (54, 55).

Statistical analysis

All statistical analyses other than RNAseq gene expression analysis was performed using GraphPad Prism 9 Software (GraphPad Software, La Jolla, CA). A *P* value of < 0.05 was considered significant.

Supplementary Materials

This PDF file includes:

Figs. S1 to S4
Tables S1 to S14

Other Supplementary Material for this manuscript includes the following:

Data file S1
MDAR Reproducibility Checklist

[View/request a protocol for this paper from Bio-protocol.](#)

REFERENCES AND NOTES

1. D. J. Gubler, *Aedes aegypti* and *Aedes aegypti*-borne disease control in the 1990s: Top down or bottom up. Charles Franklin Craig Lecture. *Am. J. Trop. Med. Hyg.* **40**, 571–578 (1989).
2. S. Bhatt, P. W. Gething, O. J. Brady, J. P. Messina, A. W. Farlow, C. L. Moyes, J. M. Drake, J. S. Brownstein, A. G. Hoen, O. Sankoh, M. F. Myers, D. B. George, T. Jaenisch, G. R. Wint, C. P. Simmons, T. W. Scott, J. J. Farrar, S. I. Hay, The global distribution and burden of dengue. *Nature* **496**, 504–507 (2013).
3. D. S. Shepard, L. Coudeville, Y. A. Halasa, B. Zambrano, G. H. Dayan, Economic impact of dengue illness in the Americas. *Am. J. Trop. Med. Hyg.* **84**, 200–207 (2011).
4. World mosquito program. vol. 2021.
5. J. P. Messina, O. J. Brady, N. Golding, M. U. G. Kraemer, G. R. W. Wint, S. E. Ray, D. M. Pigott, F. M. Shearer, K. Johnson, L. Earl, L. B. Marczak, S. Shirude, N. Davis Weaver, M. Gilbert, R. Velayudhan, P. Jones, T. Jaenisch, T. W. Scott, R. C. Reiner, S. I. Hay, The current and future global distribution and population at risk of dengue. *Nat. Microbiol.* **4**, 1508–1515 (2019).

6. V. Tricou, X. Saez-Llorens, D. Yu, L. Rivera, J. Jimeno, A. C. Villarreal, E. Dato, O. Saldana de Suman, N. Montenegro, R. DeAntonio, S. Mazara, M. Vargas, D. Mendoza, M. Rauscher, M. Brose, I. Lefevre, S. Tuboi, A. Borkowski, D. Wallace, Safety and immunogenicity of a tetravalent dengue vaccine in children aged 2-17 years: A randomised, placebo-controlled, phase 2 trial. *Lancet* **395**, 1434–1443 (2020).
7. S. Biswal, H. Reynales, X. Saez-Llorens, P. Lopez, C. Borja-Tabora, P. Kosalaraksa, C. Sirivichayakul, V. Watanaveeradej, L. Rivera, F. Espinoza, L. Fernando, R. Dietze, K. Luz, R. Venancio da Cunha, J. Jimeno, E. Lopez-Medina, A. Borkowski, M. Brose, M. Rauscher, I. LeFevre, S. Bizjajeva, L. Bravo, D. Wallace; TIDES Study Group, Efficacy of a tetravalent dengue vaccine in healthy children and adolescents. *N. Engl. J. Med.* **381**, 2009–2019 (2019).
8. B. D. Kirkpatrick, A. P. Durbin, K. K. Pierce, M. P. Carmolli, C. M. Tibery, P. L. Grier, N. Hynes, S. A. Diehl, D. Elwood, A. P. Jarvis, B. P. Sabundayo, C. E. Lyon, C. J. Larsson, M. Jo, J. M. Lovchik, C. J. Luke, M. C. Walsh, E. A. Fraser, K. Subbarao, S. S. Whitehead, Robust and balanced immune responses to all 4 dengue virus serotypes following administration of a single dose of a live attenuated tetravalent dengue vaccine to healthy, flavivirus-naive adults. *J. Infect. Dis.* **212**, 702–710 (2015).
9. B. D. Kirkpatrick, S. S. Whitehead, K. K. Pierce, C. M. Tibery, P. L. Grier, N. A. Hynes, C. J. Larsson, B. P. Sabundayo, K. R. Talaat, A. Janiak, M. P. Carmolli, C. J. Luke, S. A. Diehl, A. P. Durbin, The live attenuated dengue vaccine TV003 elicits complete protection against dengue in a human challenge model. *Sci. Transl. Med.* **8**, 330ra36 (2016).
10. M. R. Capeding, N. H. Tran, S. R. Hadinegoro, H. I. Ismail, T. Chotpitayasonondh, M. N. Chua, C. Q. Luong, K. Rusmil, D. N. Wirawan, R. Nallusamy, P. Pitisuttithum, U. Thisyakorn, I. K. Yuon, D. van der Vliet, E. Langevin, T. Laot, Y. Hutagalung, C. Frago, M. Boaz, T. A. Wartel, N. G. Tornieporth, M. Saville, A. Bouckennooghe; CYD14 Study Group, Clinical efficacy and safety of a novel tetravalent dengue vaccine in healthy children in Asia: A phase 3, randomised, observer-masked, placebo-controlled trial. *Lancet* **384**, 1358–1365 (2014).
11. L. Villar, G. H. Dayan, J. L. Arredondo-García, D. M. Rivera, R. Cunha, C. Deseda, H. Reynales, M. S. Costa, J. O. Morales-Ramírez, G. Carrasquilla, L. C. Rey, R. Dietze, K. Luz, E. Rivas, M. C. Miranda Montoya, M. Cortés Supelano, B. Zambrano, E. Langevin, M. Boaz, N. Tornieporth, M. Saville, F. Noriega, Efficacy of a tetravalent dengue vaccine in children in Latin America. *N. Engl. J. Med.* **372**, 113–123 (2015).
12. World Health Organization, Dengue vaccine: WHO position paper, July 2016 - recommendations. *Vaccine* **35**, 1200–1201 (2017).
13. S. J. F. Kaptein, O. Goethals, D. Kiemel, A. Marchand, B. Kesteley, J. F. Bonfanti, D. Bardiot, B. Stoops, T. H. M. Jonckers, K. Dallmeier, P. Geluykens, K. Thys, M. Crabbe, L. Chatel-Chaix, M. Munster, G. Querat, F. Touret, X. de Lamballerie, P. Rabaïsson, K. Simmen, P. Chaltin, R. Bartschlagler, M. Van Loock, J. Neyts, A pan-serotype dengue virus inhibitor targeting the NS3-NS4B interaction. *Nature* **598**, 504–509 (2021).
14. T. P. Endy, D. Wang, M. E. Polhemus, R. G. Jarman, L. E. Jasper, G. Gromowski, L. Lin, R. A. De La Barra, H. Friberg, J. R. Currier, M. Abbott, L. Ware, M. Klick, K. M. Polino, D. C. Blair, K. Eckels, W. Rutvisuttinunt, S. J. Thomas, A phase 1, open-label assessment of a dengue virus-1 live virus human challenge strain. *J. Infect. Dis.* **223**, 258–267 (2021).
15. H. Graham, Dengue: A study of its mode of propagation and pathology. *Med. Rec. New York* **61**, 204–207 (1902).
16. G. Harris, The dengue: A study of its pathology and mode of propagation. *J. Trop. Med.* **6**, 209–214 (1903).
17. P. Ashburn, C. Craig, Experimental investigations regarding the etiology of dengue fever. *J. Infect. Dis.* **4**, 440–475 (1907).
18. J. B. Cleland, B. Bradley, W. Macdonald, Further experiments in the etiology of dengue fever. *J. Hyg.* **18**, 217–254 (1919).
19. J. F. Siler, M. W. Hall, A. P. Hitchens, Dengue: Its history, epidemiology, mechanism of transmission, etiology, clinical manifestations, immunity, and prevention, in *Philippine Islands Bureau of Science Monograph 20* (Bureau of Printing, Manila, 1926).
20. J. S. Simmons, J. H. St. John, F. Reynolds, *Experimental Studies of Dengue* (Bureau of Printing, Manila, 1931).
21. T. Sawada, H. Sato, S. Sai, On the experimental dengue infection in man. *Nippon Igaku* **332A**, 529–531 (1943).
22. A. B. Sabin, R. W. Schlesinger, Production of immunity to dengue with virus modified by propagation in mice. *Science* **101**, 640–642 (1945).
23. S. Hotta, Experimental studies on dengue. I. Isolation, identification and modification of the virus. *J. Infect. Dis.* **90**, 1–9 (1952).
24. A. B. Sabin, Research on dengue during World War II. *Am. J. Trop. Med. Hyg.* **1**, 30–50 (1952).
25. H. Yaoi, A summary of our studies on dengue. *Yokohama Med. Bull.* **9**, 1–20 (1958).
26. A. T. Waickman, H. Friberg, G. D. Gromowski, W. Rutvisuttinunt, T. Li, H. Siegfried, K. Victor, M. K. McCracken, S. Fernandez, A. Srikiatkachorn, D. Ellison, R. G. Jarman, S. J. Thomas, A. L. Rothman, T. Endy, J. R. Currier, Temporally integrated single cell RNA sequencing analysis of PBMC from experimental and natural primary human DENV-1 infections. *PLoS Pathog.* **17**, e1009240 (2021).
27. J. P. Hanley, H. A. Tu, J. A. Dragon, D. M. Dickson, R. D. Rio-Guerra, S. W. Tighe, K. M. Eckstrom, N. Selig, S. V. Scarpino, S. S. Whitehead, A. P. Durbin, K. K. Pierce, B. D. Kirkpatrick, D. M. Rizzo, S. F. Fretz, S. A. Diehl, Immunotranscriptomic profiling the acute and clearance phases of a human challenge dengue virus serotype 2 infection model. *Nat. Commun.* **12**, 3054 (2021).
28. A. Grifoni, M. Angelo, J. Sidney, S. Paul, B. Peters, A. D. de Silva, E. Phillips, S. Mallal, S. A. Diehl, J. Botten, J. Boyson, B. D. Kirkpatrick, S. S. Whitehead, A. P. Durbin, A. Sette, D. Weiskopf, Patterns of cellular immunity associated with experimental infection with rDEN2Δ30 (Tonga/74) support its suitability as a human dengue virus challenge strain. *J. Virol.* **91**, (2017).
29. P. M. Repik, J. M. Dalrymple, W. E. Brandt, J. M. McCown, P. K. Russell, RNA fingerprinting as a method for distinguishing dengue 1 virus strains. *Am. J. Trop. Med. Hyg.* **32**, 577–589 (1983).
30. K. T. McKee Jr., W. H. Bancroft, K. H. Eckels, R. R. Redfield, P. L. Summers, P. K. Russell, Lack of attenuation of a candidate dengue 1 vaccine (45A25) in human volunteers. *Am. J. Trop. Med. Hyg.* **36**, 435–442 (1987).
31. A. D. Wegman, H. Fang, A. L. Rothman, S. J. Thomas, T. P. Endy, M. K. McCracken, J. R. Currier, H. Friberg, G. D. Gromowski, A. T. Waickman, Monomeric IgA antagonizes IgG-mediated enhancement of DENV infection. *Front. Immunol.* **12**, 777672 (2021).
32. A. T. Waickman, G. D. Gromowski, W. Rutvisuttinunt, T. Li, H. Siegfried, K. Victor, C. Kuklis, M. Gomootsukavadee, M. K. McCracken, B. Gabriel, A. Mathew, I. E. A. Grinyo, M. E. Fouch, J. Liang, S. Fernandez, E. Davidson, B. J. Doranz, A. Srikiatkachorn, T. Endy, S. J. Thomas, D. Ellison, A. L. Rothman, R. G. Jarman, J. R. Currier, H. Friberg, Transcriptional and clonal characterization of B cell plasmablast diversity following primary and secondary natural DENV infection. *EBioMedicine* **54**, 102733 (2020).
33. G. Winkler, S. E. Maxwell, C. Ruemmler, V. Stollar, Newly synthesized dengue-2 virus non-structural protein NS1 is a soluble protein but becomes partially hydrophobic and membrane-associated after dimerization. *Virology* **171**, 302–305 (1989).
34. M. J. Pryor, P. J. Wright, The effects of site-directed mutagenesis on the dimerization and secretion of the NS1 protein specified by dengue virus. *Virology* **194**, 769–780 (1993).
35. L. A. Sanchez Vargas, A. Adam, M. Masterson, M. Smith, Z. L. Lyski, K. A. Dowd, T. C. Pierson, W. B. Messer, J. R. Currier, A. Mathew, Non-structural protein 1-specific antibodies directed against Zika virus in humans mediate antibody-dependent cellular cytotoxicity. *Immunology* **164**, 386–397 (2021).
36. K. M. Chung, B. S. Thompson, D. H. Fremont, M. S. Diamond, Antibody recognition of cell surface-associated NS1 triggers Fc-gamma receptor-mediated phagocytosis and clearance of West Nile virus-infected cells. *J. Virol.* **81**, 9551–9555 (2007).
37. I. Kurane, T. Matsutani, R. Suzuki, T. Takasaki, S. Kalayanaraj, S. Green, A. L. Rothman, F. A. Ennis, T-cell responses to dengue virus in humans. *Trop. Med. Health* **39**, 45–51 (2011).
38. A. T. Waickman, H. Friberg, M. Gargulak, A. Kong, M. Polhemus, T. Endy, S. J. Thomas, R. G. Jarman, J. R. Currier, Assessing the diversity and stability of cellular immunity generated in response to the candidate live-attenuated dengue virus vaccine TAK-003. *Front. Immunol.* **10**, 1778 (2019).
39. M. Robinson, T. E. Sweeney, R. Barouch-Bentov, M. K. Sahoo, L. Kalesinskas, F. Vallania, A. M. Sanz, E. Ortiz-Lasso, L. L. Albornoz, F. Rosso, J. G. Montoya, B. A. Pinsky, P. Khatri, S. Einav, A 20-gene set predictive of progression to severe dengue. *Cell Rep.* **26**, 1104–1111.e4 (2019).
40. K. Alagarasu, A. M. Walimbe, S. M. Jadhav, A. R. Deoshwar, A meta-analysis of the diagnostic accuracy of dengue virus-specific IgA antibody-based tests for detection of dengue infection. *Epidemiol. Infect.* **144**, 876–886 (2016).
41. P. Koraka, C. Suharti, T. E. Setiati, A. T. Mairuhu, E. Van Gorp, C. E. Hack, M. Juffrie, J. Sutaryo, G. M. Van Der Meer, J. Groen, A. D. Osterhaus, Kinetics of dengue virus-specific serum immunoglobulin classes and subclasses correlate with clinical outcome of infection. *J. Clin. Microbiol.* **39**, 4332–4338 (2001).
42. R. Bachal, K. Alagarasu, A. Singh, A. Salunke, P. Shah, D. Cecilia, Higher levels of dengue-virus-specific IgG and IgA during pre-defervescence associated with primary dengue hemorrhagic fever. *Arch. Virol.* **160**, 2435–2443 (2015).
43. A. A. Berry, J. M. Obiero, M. A. Travassos, A. Ouattara, D. Coulibaly, M. Adams, R. R. de Assis, A. Jain, O. Taghavian, A. Sy, R. Nakajima, A. Jasinskas, M. B. Laurens, S. Takala-Harrison, B. Kouriba, A. K. Kone, O. K. Doumbo, B. K. L. Sim, S. L. Hoffman, C. V. Plowe, M. A. Thera, P. L. Felgner, K. E. Lyke, Immunoprofiles associated with controlled human malaria infection and naturally acquired immunity identify a shared IgA pre-erythrocytic immunoproteome. *NPJ Vaccines* **6**, 115 (2021).
44. L. Azzi, D. Dalla Gasperina, G. Veronesi, M. Shallak, G. Ietto, D. Iovino, A. Baj, F. Gianfagna, V. Maurino, D. Focosi, F. Maggi, M. M. Ferrario, F. Dentali, G. Carcano, A. Tagliabue, L. S. Maffioli, R. S. Accolla, G. Forlani, Mucosal immune response in BNT162b2 COVID-19 vaccine recipients. *EBioMedicine* **75**, 103788 (2021).
45. B. Puri, W. M. Nelson, E. A. Henchal, C. H. Hoke, K. H. Eckels, D. R. Dubois, K. R. Porter, C. G. Hayes, Molecular analysis of dengue virus attenuation after serial passage in primary dog kidney cells. *J. Gen. Virol.* **78** (Pt 9), 2287–2291 (1997).

46. H. S. Hounq, R. Chung-Ming Chen, D. W. Vaughn, N. Kanesa-thasan, Development of a fluorogenic RT-PCR system for quantitative identification of dengue virus serotypes 1-4 using conserved and serotype-specific 3' noncoding sequences. *J. Virol. Methods* **95**, 19–32 (2001).
47. N. L. Bray, H. Pimentel, P. Melsted, L. Pachter, Erratum: Near-optimal probabilistic RNA-seq quantification. *Nat. Biotechnol.* **34**, 888 (2016).
48. C. Sonesson, M. I. Love, M. D. Robinson, Differential analyses for RNA-seq: Transcript-level estimates improve gene-level inferences. *F1000Res* **4**, 1521 (2015).
49. M. D. Robinson, D. J. McCarthy, G. K. Smyth, edgeR: A Bioconductor package for differential expression analysis of digital gene expression data. *Bioinformatics* **26**, 139–140 (2010).
50. D. J. McCarthy, Y. Chen, G. K. Smyth, Differential expression analysis of multifactor RNA-Seq experiments with respect to biological variation. *Nucleic Acids Res.* **40**, 4288–4297 (2012).
51. M. E. Ritchie, B. Phipson, D. Wu, Y. Hu, C. W. Law, W. Shi, G. K. Smyth, limma powers differential expression analyses for RNA-sequencing and microarray studies. *Nucleic Acids Res.* **43**, e47 (2015).
52. L. Kolberg, U. Raudvere, I. Kuzmin, J. Vilo, H. Peterson, gprofiler2—An R package for gene list functional enrichment analysis and namespace conversion toolset g:Profiler. *F1000Res* **9**, ELIXIR-709 (2020).
53. A. M. Bolger, M. Lohse, B. Usadel, Trimmomatic: A flexible trimmer for Illumina sequence data. *Bioinformatics* **30**, 2114–2120 (2014).
54. D. A. Bolotin, S. Poslavsky, I. Mitrophanov, M. Shugay, I. Z. Mamedov, E. V. Putintseva, D. M. Chudakov, MiXCR: Software for comprehensive adaptive immunity profiling. *Nat. Methods* **12**, 380–381 (2015).
55. D. A. Bolotin, S. Poslavsky, A. N. Davydov, F. E. Frenkel, L. Fanchi, O. I. Zolotareva, S. Hemmers, E. V. Putintseva, A. S. Obratsova, M. Shugay, R. I. Ataulkhanov, A. Y. Rudensky, T. N. Schumacher, D. M. Chudakov, Antigen receptor repertoire profiling from RNA-seq data. *Nat. Biotechnol.* **35**, 908–911 (2017).

Acknowledgments: We acknowledge the excellent technical assistance provided by K. Gentile of the Upstate Medical University Molecular Analysis Core (MAC) and the members of the Institute for Global Health and Translational Science (IGHTS) of the SUNY Upstate Medical

University. We also acknowledge LTC R. Jarman and C. Rooney from the U.S. Army and the members of the dengue research team at Janssen Pharmaceutica. We also wish to thank all the study participants for making this study possible. The following reagents were obtained through BEI Resources, NIAID, NIH: Peptide Array, DENV-1 Singapore/S275/1990 E protein (NR-50710), DENV-1 Singapore/S275/1990 NS1 protein (NR-2751), DENV-1 Singapore/S275/1990 NS3 protein (NR-2752), and DENV-1 Singapore/S275/1990 NS5 protein (NR-4203). The opinions or assertions contained here are the private views of the authors and are not to be construed as reflecting the official views of the U.S. Army or the U.S. Department of Defense. Material has been reviewed by the Walter Reed Army Institute of Research. There is no objection to its presentation and/or publication. The investigators have adhered to the policies for protection of human participants as prescribed in AR 70-25. **Funding:** Funding for this research was provided by Janssen Pharmaceutica NV, the State of New York, and the Congressionally Directed Medical Research Program. **Author contributions:** L.W., L.V.W., N.V., O.L., L.T., G.H.-T., M.V.L., T.P.E., and S.J.T. designed the study and interpreted the data. J.Q.L. performed serologic and virologic assays. H.F. performed virologic and cellular immunology assays. M.J.W. and C.G. performed serologic assays. J.R.C. developed methodologies and reagents. A.T.W. analyzed and interpreted the data. A.T.W. and S.J.T. wrote the paper with assistance from all coauthors. **Competing interests:** L.V.W., O.L., L.T., G.H.-T., and M.V.L. are employees and shareholders of Johnson and Johnson. All other authors declare that they have no competing interests. **Data and materials availability:** All data needed to evaluate the conclusions in the paper are present in the paper and/or the Supplementary Materials or from the corresponding author upon reasonable request. RNAseq gene expression data have been deposited in the Gene Expression Omnibus database under the accession code GSE182482. The DENV strain used for this study was made available by the U.S. Army Medical Research and Development Command under a material transfer agreement with the SUNY Upstate Medical University and SUNY Research Foundation, to whom requests for the challenge strain should be addressed.

Submitted 11 February 2022

Accepted 6 October 2022

Published 26 October 2022

10.1126/scitranslmed.abo5019

Abstract

One-sentence summary: This study provides a high-resolution analysis of the virologic and immunologic features of primary dengue in flavivirus naïve individuals.

Editors's Summary

A human model of dengue virus infection

Dengue virus (DENV) infections have a marked impact on morbidity and mortality in subtropical and tropical regions with endemic disease. Immune response vary widely to different DENV serotypes and are not well understood. Waickman *et al.* used a DENV human infection model to characterize virologic and immunologic features of early infection to better understand these early responses to an attenuated DENV-1 strain. They detected a notable DENV-specific IgA Ab response between characteristic IgM and IgG responses, and an NS1-specific Ab response was detected after the appearance of DENV virion-specific Abs. They also characterized transcriptional profiles that correlated with acute viremia and initiation of adaptive immune responses. These findings provide detailed immunological data during early DENV infection in humans that has the potential to improve the development of therapeutic and vaccine-based approaches.